
SUNMASK: Mask Enhanced Control in Step Unrolled Denoising Autoencoders

Anonymous Author(s)

Affiliation

Address

email

Abstract

1 This paper introduces SUNMASK, an approach for generative sequence modeling
2 based on masked unrolled denoising autoencoders. By explicitly incorporating a
3 conditional masking variable, as well as using this mask information to modulate
4 losses during training based on expected exemplar difficulty, SUNMASK models
5 discrete sequences without direct ordering assumptions. The addition of masking
6 terms allows for fine-grained control during generation, starting from random
7 tokens and a mask over subset variables, then predicting tokens which are again
8 combined with a subset mask for subsequent repetitions. This iterative process
9 gradually improves token sequences toward a structured output, while guided by
10 proposal masks. The broad framework for unrolled denoising autoencoders is
11 largely independent of model type, and we utilize both transformer and convolution
12 based architectures in this work. We demonstrate the efficacy of this approach both
13 qualitatively and quantitatively, applying SUNMASK to generative modeling of
14 symbolic polyphonic music, and language modeling for English text.

15 1 Introduction

16 Generative modeling approaches can stratified into different modeling approaches based on factoriza-
17 tion to form two broad categories, autoregressive modeling (AR) and non-autoregressive modeling
18 (NAR). We introduce SUNMASK, a NAR generative model for structured sequences.

19 1.1 Autoregressive Models

20 AR modeling with deep neural networks has been a dominant approach to generative modeling
21 and feature learning [38, 70, 73, 39, 76, 74] which has many crucial advantages in both training
22 and inference. One key concern is the necessity of defining a "dependency chain" in the form of
23 a (typically) directed acyclic graph (DAG). Sampling during inference can be accomplished in a
24 straightforward manner using ancestral sampling - sampling from the first variable or variables in the
25 DAG, using those to conditionally estimate a probability distribution for subsequent variables.

26 Many applications have straightforward orderings in which to define this chain of variables, based
27 on domain knowledge. For example following the flow of time for timeseries modeling is often
28 a logical choice, allowing models to make predictions into the future from the past. However in
29 many other domains, for example images, language, or music, the process of defining a dependency
30 chain over input variables (e.g. pixels, characters, words, or notes) is far from straightforward, as
31 for any arbitrary ordering there can frequently be examples where this ordering *creates* long-term
32 dependencies, or otherwise makes satisfaction of dependencies during training and evaluation more
33 difficult than another alternative ordering.

34 This divide becomes further compounded in many creative applications to these domains, as creators
35 typically iterate repeatedly: forming a concept, applying an initial sequence of steps to create the

36 framing of the concept, and seeing where the creative flow may lead to alterations in the original
37 concept, thus altering future steps. Though the resulting output may be perceived in a time-ordered
38 fashion (for example, reading a book or listening to a song), the initial creation was performed
39 globally and holistically. This global view is often critical to creating elements such as foreshadowing
40 and tension which make the resulting output interesting or enjoyable. This iterative process is directly
41 at odds with a strict AR factorization, and requires well trained AR models to cope with a high degree
42 of uncertainty and multi-modality for long range dependencies, which can lead to logical mistakes or
43 other errors.

44 1.2 Non-Autoregressive Models

45 An alternative methodology for generative modeling is non-autoregression (NAR), broadly covering a
46 large number of different modeling approaches which attempt to remove assumptions about variable
47 ordering, instead either hand-defining per-exemplar orderings, or modeling variables jointly without
48 resorting to chain rule factorization. One way to define an ordering over variables is via masking
49 of inputs or intermediate network representations [22, 71, 72, 77, 73, 57], and indeed modern AR
50 approaches such as transformers [75] use an autoregressive mask internally to define the chain of
51 variables order. These masks can either be constant over all training (as in standard AR transformers
52 and PixelCNN [73]) or dynamic per example (as in MADE [22]). When masks are dynamic per
53 example, we begin to see the relationship between enforcing AR via masking and NAR methods, as
54 although some ordering is assumed this ordering is no longer constant, and it becomes possible to
55 use the same trained model to evaluate the probability of a particular output variable under *multiple*
56 possible orderings.

57 Closely linked to masking methods are so called *diffusion models*, which relax the variable ordering
58 problem through noise prediction [67, 69, 30]. Rather than predicting a new variable or variables
59 given previous ones in an arbitrarily chosen DAG, diffusion models focus on predicting a less
60 noisy version of many variables jointly, given a set of noisy input variables. Iteratively applying
61 this learned denoising improvement operator should eventually result in predicting a fully clean
62 output estimate, given either a noisy version of the target domain, or even starting from pure noise.
63 Given this framing it is clear that diffusion models are closely linked to denoising methods in
64 general, specifically denoising autoencoders, as well as modern density modeling approaches such
65 as generative adversarial networks (GAN [23]), variational autoencoders (VAE [41]), flow-based
66 models (NICE [15], RealNVP [16], Normalizing Flows [61], IAF [42], MAF [57]), iterative canvas
67 sampling (DRAW [24]), and noise contrastive estimation (NCE [27]). Particular applications of
68 this denoising philosophy such as BERT [14], WaveGrad [9], and GLIDE [56], have resulted in
69 large quality improvements for feature learning and data generation for text, images, and audio
70 [46, 66, 60, 29].

71 1.3 Trade-offs Between AR and NAR Approaches

72 The choice between AR and NAR methods is not clear-cut. For many domains, high-quality models
73 exist using both approaches but we can define some crucial parameters. Some NAR methods such as
74 GAN or VAE are capable of generating output in only one inference step, however they are typically
75 hard to train on certain data modalities (e.g. text data) comparing to AR counterparts. Other NAR
76 methods such as diffusion models typically allow for choosing a diffusion length during inference,
77 which is independent of that used at training. Choosing a low diffusion length can frequently lead to
78 poor sample quality, and tuning this setting (among many others) is critical to high quality generation.
79 However if the tuned diffusion length for a given sequence (of length T) is shorter than the length
80 of those sequences, the NAR method has a computational advantage over the equivalent AR model
81 (which would require T steps for a T length sequence). In addition, the ability to tune this diffusion
82 length can be useful in interactive applications, or when a variety of output is desirable. This
83 setting can also be a curse, as even well-trained models perform poorly with improper diffusion
84 settings. Several branches of current research are focused on improving guarantees [35, 68, 40] and
85 convergence speed for diffusion models [43, 44, 36, 79].

86 1.4 SUNMASK, a non-autoregressive sequence model

87 We introduce SUNMASK, a NAR sequence model which uses masks over noised, discrete data
88 to learn a self-improvement operator to transition from categorical noise to the data distribution in

89 iterated steps. Given a target data representation, we train a model which can map from a noisy
 90 version of input data to a corrected form of the input. In this work, we use multinomial noise - namely
 91 entries are corrupted to 1 of P possible values (for a given set size P), with the number of noised
 92 entries defining the relative noise level for the training example. This is similar to many diffusion
 93 approaches at a high level, and particularly shown to be an effective tool in SUNDAE [65] and
 94 Coconet [33]. In addition to the use of multinomial noise, we also form a mask representing *where*
 95 the data was noised, feeding this mask alongside the input data to form a conditional probability
 distribution.

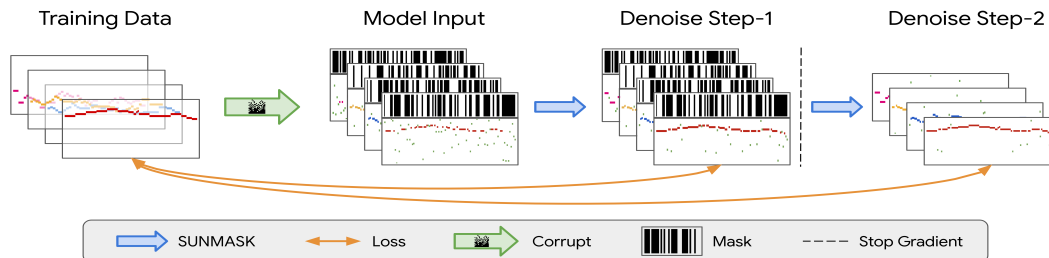


Figure 1: Step-unrolled denoising training for SUNMASK on polyphonic music, unrolled step length 2. Training data (left) consists of four voices corrupted by sampling a random mask per voice and replacing the masked data (red) with random pitches (green). SUNMASK takes both mask and corrupted training data as input, predicting denoised original data as output. In the second step, the model takes a sampled version of the model step predictions and the same mask as input, outputting another prediction of the original data.

97 2 Method

98 The relationship between discrete diffusion and denoising autoencoders has been explored in previous
 99 work [31, 65, 3, 32]. We build upon this foundation, combined with many insights from prior
 100 orderless modeling approaches, crucially Orderless NADE [72], Coconet [33] (which is a more
 101 modern variant of Orderless NADE), and SUNDAE [65].

102 SUNMASK is built around a process $x_t \sim f_\theta(\cdot|x_{t-1}; m)$ on a space $X = \{1, \dots, v\}^N$ of arrays of
 103 categorical variables. This parametric transition function f_θ takes an additional argument $m \in 0, 1^N$.
 104 During training, m indicates variables that were not corrupted, and as a consequence we can use it
 105 during inference to tell f_θ which variables to trust.

106 Given a sequence of masks m_0, \dots, m_{T-1} , the generating distribution of our model derives from a
 107 prior p_0 (typically uniform noise) and repeated application of f_θ :

$$p_T(x_T; m_0, \dots, m_{T-1}) = \left(\sum_{x_1, \dots, x_{T-1} \in X} \prod_{t=1}^T f_\theta(x_t|x_{t-1}; m_{t-1}) \right) p_0(x_0) \quad (1)$$

108 In practice, p_0 is typically elementwise iid uniform noise, and the masks m_0, \dots, m_{T-1} are drawn
 109 according to a schedule and may be held constant for several steps.

110 To train f_θ , we take a training example $x \sim p_{\text{data}}$ and draw a mask m . We apply the corruption
 111 procedure $x_0 \sim q(\cdot|x; m)$ to obtain x_0 which equals x where the mask m is true and uniform random
 112 values elsewhere. Then we iterate $x_t \sim f_\theta(\cdot|x_{t-1}; m)$ with the aim of reconstructing x .

113 As in SUNDAE, the transition f_θ models the variables as conditionally independent of one another.
 114 However SUNDAE has no direct concept of masking. SUNMASK thus combines past insights from
 115 the masked NAR models Orderless NADE and Coconet with existing concepts from SUNDAE, along
 116 with new model classes and inference schemes to form a powerful generative model. Similar to
 117 SUNDAE, our objective is to minimize $\frac{1}{2}(L^{(1)} + L^{(2)})$ where

$$L^{(i)}(\theta) = -\mathbb{E}_{m_0, \dots, m_{t-1}} \mathbb{E}_{\substack{x \sim p_{\text{data}} \\ x_0 \sim q(\cdot|x, m_0) \\ x_1 \sim f_\theta(\cdot|x_0; m_0) \\ x_2 \sim f_\theta(\cdot|x_1; m_1) \\ \dots \\ x_{t-1} \sim f_\theta(\cdot|x_{t-2}; m_{t-2})}} \left[\frac{\sum_i (1 - m_{t-1}^{(i)}) \log f_\theta^{(i)}(x^{(i)}|x_{t-1}; m_{t-1})}{\sum_i 1 - m_{t-1}^{(i)}} \right] \quad (2)$$

118 is the reconstruction loss for the elements of x that were corrupted. As in Orderless NADE [72]
 119 and Coconet [33], we weigh each term according to the size of the mask, to ensure that the overall
 120 weight on each conditional $f_{\theta}^{(i)}$ is uniform across i . Unlike previous methods, we target *only masked*
 121 *variables* in the loss. In practice we choose $m_0 = \dots = m_{t-1}$ during training and $t = 2$. Since we
 122 only go to $t = 2$, keeping the mask constant is a close enough approximation to the masking schedule
 123 used in inference. The choice of $t = 2$ is driven by the ablation study in SUNDAE, where $t = 2$ was
 124 found to account for nearly all performance gains in translation experiments, with higher unrollings
 125 showing no additional benefit. In addition higher values of t unrolling generally increase memory
 126 usage, making the training of high order unrollings complicated.

127 Coupled with multi-step unrolling, the SUNMASK training scheme encourages learning complex
 128 relationships between the mask and the data, allowing the potential for multi-level trust over the input
 129 data: variables with a mask value of 1 which appear correct (given context), variables of mask value 1
 130 which appear incorrect, variables of mask value 0 which appear correct, and variables of mask value
 131 0 which appear incorrect. Denoising only methods (such as SUNDAE [65]) would need to form
 132 an internal, non-controllable mask in order to disentangle these states, and 0 mask models (such as
 133 Coconet [33]) have controllable input masks but combine both masked states.

134 SUNMASK allows for direct control at inference using both proposal masks and noising of variables,
 135 combining elements of both SUNDAE and Coconet. We show a high level example of the unrolled
 136 training scheme, mask proposals, and input data processing in Figure 1.

137 2.1 SUNMASK, SUNDAE, and Coconet Comparison

138 The overall unrolled mask and iterative inference setting is largely independent of architecture choice,
 139 and as long as the internal architecture does not make any ordering assumption over the input data
 140 we can incorporate it into SUNMASK. We use two primary archetypes for the internal model in
 141 this paper: Attentional U-Net and Relative Transformer. Detailed description of the respective
 142 architectures can be seen in the Appendix.

143 SUNMASK uses an unrolled training scheme, similar to that shown in SUNDAE, as well as a mask
 144 which is input to the model and defines manipulated variables as in Coconet. The loss is masked based
 145 on this manipulation mask, unlike Coconet or SUNDAE. The SUNMASK loss is further weighted by
 146 the total amount of masked variables. Comparisons of various high level modeling features between
 147 SUNMASK, Coconet, and SUNDAE are shown in Table 1.

Table 1: Comparison of model features for
 SUNMASK, Coconet, and SUNDAE

Model	SUNMASK	Coconet	SUNDAE
Mask input to model	✓	✓	X
Masked loss	✓	X	X
Re-weighted loss	✓	✓	X
Unrolled loss	✓	X	✓
Inference mask schedule	✓	✓	X
Sampling rejection step	✓	X	✓
Mask control preserves data	✓	X	X

148 2.2 Model Training

149 During training, the internal architecture is combined with a *step unrolled* training procedure, as
 150 highlighted by SUNDAE [65]. Rather than directly randomizing positions, we re-write this as a
 151 masking scheme, first sampling a mask (with 0 randomize, 1 keep, which we denote as 0-active
 152 format) then performing randomization to one of P possibilities, for the masked subset of K variables.
 153 This random masking procedure is equivalent to the approach from SUNDAE, but using a mask
 154 allows us to further combine the mask information with the input data, in order to form a conditional
 155 probability estimate. In addition, this 0-active masking scheme makes direct comparison to masking
 156 schemes with absorbing states (such as OrderlessNADE [72], Coconet [33], VQ-Diffusion [25] and
 157 OA-ARDM [31]) simpler, as the mask can be directly multiplied with the data in a 0-active format.

158 Convolutional SUNMASK incorporates mask information with a one-hot data representation by
 159 concatenation along the channel axis. Transformer SUNMASK uses a slightly different setting -

160 assuming input transformer data (T, B) , with T timesteps, B batch elements, and vocabulary size P
161 is transformed to a (T, B, L) dimensional embedding, we repeat the mask along the embedding axis
162 L times, downweighting the values in the mask by $\frac{1}{\sqrt{L}}$ for numerical reasons. Concatenating this
163 reduced mask with the input embedding along the last axis is sufficient to form the desired conditional
164 probability distribution. This stretched and reduced mask format provides more stable training than
165 other schemes such as separately embedding the mask, then concatenating or summing with the input
166 data embedding.

167 Each training batch is randomly sampled from the training dataset, and a corresponding noise value
168 drawn from $rand(N)$ for N examples in the minibatch. This per-example noise value is then used
169 to derive a per-step mask over T timesteps, by comparing noise $rand(N) < rand(N, T)$. During
170 training, this means some examples have a high per-example noise value (e.g. .99), and thus many
171 values masked and noised in the training, while other examples may have a low noise value (e.g.
172 .01) drawn instead. Combined with a training loss which learns to denoise the input and focuses on
173 imputing information about masked corrupted inputs, the overall model will learn a chain to go from
174 more noisy data to less noisy step-wise, resulting in a learned improvement operator [32, 65].

175 This improvement operator can be applied to noisy data or pure noise, and iterate toward a predictive
176 sample from the training distribution. See Multinomial Diffusion [32] and SUNDAE [65] for more
177 detail on this proof, as well as fundamental work on denoising autoencoders [1]. In SUNMASK, we
178 combine the mask used to noise the input with the input data itself, while modifying the loss to predict
179 *only masked variables*. In addition, we downweight the loss by $\frac{1}{1+\sum 1-m_t}$ for each batch element,
180 meaning that losses for heavily masked entries are downweighted compared to losses on examples
181 with little masking, in a form of curriculum weighting based on expected estimation difficulty.

182 While a one step denoising scheme can be sufficient for learning the data manifold [3, 1], *unrolling*
183 this denoising scheme into a multi-step process can have performance benefits. SUNMASK directly
184 uses the unrolled loop scheme described in [65], using a step value of 2. For a detailed description of
185 the step unrolled training scheme, see Appendix or the overview description from SUNDAE [65].
186 The masked and unrolled training can be seen as a container for any internal model which does
187 not make ordering assumptions, and we utilize both convolutional U-Net (a variant of GLIDE [56]
188 U-Net) and Relative Transformer [12, 34, 59] models for various experiments, shown in Section 4.

189 2.3 Inference Specific Settings

190 Well-trained SUNMASK models should be applicable to full content generation, as well as a variety
191 of partially conditional generative tasks such as infilling and human-in-the-loop creation. Basic
192 sampling involves creating a set of variables, with all variables randomly set to 1 of P values in the
193 domain (or partial randomization in the case of infilling) along with an accompanying mask, which is
194 initially all 0 for full generation, or mixed 1s and 0s for partial generation tasks. Given this data and
195 mask as input, the trained model then predicts a probability distribution over all possible P values, for
196 all variables. Despite the use of masked losses in training, we sample these prediction distributions
197 for *all* variables. These predictions are then accepted or rejected from the original set, resulting in a
198 new variable set. We then sample a new mask (based on a predefined schedule) and combine it with
199 the initial mask, then iterate this overall process, updating at least some of the variables at each step.

200 During inference we use several key techniques to improve generative quality. We use typicality
201 sampling [52] on the output probability distribution and a variable number of diffusion steps, on
202 the order of 100 to 2000. Masks are randomly sampled using the schedule defined in [33] which
203 linearly decreases the number of masked variables over time according to $\alpha_n = \max(\alpha_{\min}, \alpha_{\max} -$
204 $\frac{n}{\eta N}(\alpha_{\max} - \alpha_{\min}))$ with $\alpha_{\min} = .001$, $\alpha_{\max} = .999$, and $\eta = 3/4$ as in [33], along with an optional
205 triangular linear ramp-up and ramp-down schedule for the probability of accepting predictions from
206 the model into the current variable set at each step, as shown in [65]. Active balance, by increasing
207 the probability of updating variables which have been updated less often, is another inference time
208 option. Variables can also be re-noised at any step, randomly resetting any variable with a 0 value
209 for the mask at that diffusion step. Some problems (primarily symbolic music modeling) showed
210 increased variability from active balance and re-noising, but the usefulness of these options is task
211 dependent.

212 We caution that tuning hyperparameters for inference is critical to success, as improper settings can
213 drastically lower the performance of SUNMASK, see Section 4 for variance over various inference

214 settings in different tasks. For human-in-the-loop applications, the existence of these controls can
215 allow a number of fine-grained workflows to emerge, driven by expert users to create and curate
216 interesting output [18, 11], demonstrated in Figure 3.

217 **3 Related Work**

218 We state here some key related approaches, as well as how our method differentiates from these
219 previous settings. A number of recent publications on diffusion models and feature learning have
220 incorporated masks as part of their overall training scheme [31, 7, 29], however these papers use
221 masks for blanking, rather than as indicators over stochastic variables. Many infilling models [17,
222 37, 14, 50, 10], and masked image models [29] feature conditional modeling with a mask (blank)
223 token, predicting the variables masked from the input for feature learning or generative modeling.
224 XLNet [77] combines the infilling and autoregressive paradigms, learning arbitrary permuted orders
225 over masked out variables, using blank-out masking and randomly generated autoregressive ordering
226 similar to OrderlessNADE and Coconet. Conditional diffusion generators [53, 63, 64] and GAN
227 generators [20] have the combination of mask indicators as well as preserving stochasticity of the
228 masked variables. However these methods do not use an unrolled training scheme, and generally
229 target image related tasks, with the notable exception of maskGAN. Many models use a concept of a
230 working canvas, and do repeated inference steps for generation or correction of data [24, 4, 45, 21,
231 55], SUNMASK differs from these models due to architecture choices, training scheme, and loss
232 weighting, as well as application domain [54, 58, 62, 25, 56, 60].

233 **3.1 Convolutional SUNMASK**

234 SUNMASK is most closely related to coconet [33] and SUNDAE [65]. Coconet (as an instance of
235 OrderlessNADE), trains by sampling a random mask per training example, using this mask to set
236 part of the input (in one hot format) to zero. The mask is further concatenated to the zeroed data
237 along the channel axis, and this combined batch is passed through a deep convolutional network
238 with small 3×3 kernels. Convolutional SUNMASK uses a downweighted loss over only variables
239 masked in the input. However, SUNMASK additionally uses the unrolled training scheme, as well as
240 a different inference procedure due to preserving the values of masked out variables during training
241 and sampling.

242 Our best performing convolutional SUNMASK architecture takes hints from recent image transformer
243 and vector quantized generators, exchanging the small kernels used in Coconet for extremely large
244 kernels of shape $4 \times P$ over the time and feature dimensions, somewhat analogous to input patches,
245 removing the model’s translation invariance over the feature axis by setting kernel dimension equal
246 to the total feature size. However this makes the number of parameters per convolutional layer
247 extremely large. Convolutional SUNMASK adopts an attentional U-Net structure which reduces only
248 across the time axis, modified from GLIDE [56], rather than the deep residual convolution network
249 used by Coconet. Combined with the addition of step unrolled training, we are only able to train
250 convolutional SUNMASK with a batch size of 1 (expanded to effective batch size 2 due to step
251 unrolling) on commodity GPU hardware with 16GB VRAM.

252 Due to the design choice of extremely large kernel sizes which depend on the size of the domain, we
253 only use convolutional SUNMASK for polyphonic music experiments, see Section 4 for more details.
254 Exact specification of the convolutional U-Net architecture can be seen in the Appendix.

255 **3.2 Transformer SUNMASK**

256 Transformer SUNMASK relates closely to the transformer used in SUNDAE. The architecture uses a
257 relative multi-head attention [12, 34] and has no autoregressive masking. SUNMASK transformer
258 also uses larger batch sizes, typically 20 or larger, though this is far smaller than the batch sizes
259 seen in the experiments of SUNDAE. Sequence length and data iterator strategy were both a critical
260 aspect for training transformer SUNMASK. We found short sequences (from 32 to 128) worked best,
261 along with iteration strategies that were example based. In the language experiments, padding each
262 example to some max length resulted in more stable training than the typical language modeling
263 approach of treating the corpus as one long sequence and slicing into even sized chunks, or iterating
264 sequentially. The stability gap between padded sequences and non-overlapping chunking became
265 especially apparent at sequence lengths above 128 with transformer SUNMASK.

Table 2: Quantitative results from the Bach Mock grading function [19].
Lower values represent better chorales.

Model	Note	Rhythm	Parallel Errors	Harmonic Quality	S Intervals	A Intervals	T Intervals	B Intervals	Repeated Sequence	Overall
Bach GT	0.24 ±0.15	0.23±0.14	0.0±0.69	0.41±0.2	0.47±0.28	0.49±0.22	0.53±0.24	0.69±0.4	1.29±0.88	4.91±1.63
BachMock	0.37±0.22	0.26±0.14	2.16±3.22	0.54±0.31	0.53±0.35	0.71±0.34	0.73±0.38	0.89±0.68	1.86±2.81	8.94±4.64
SMc-T-BEST20-200 AugGen	0.39±0.16	0.53±0.26	0.0±0.81	0.68±0.27	0.59±0.25	0.88±0.42	0.80±0.20	0.71±0.27	1.44±0.52	7.16±0.97 8.02±2.92
Coconet	0.44±0.23	1.85±0.39	2.61±6.56	1.38±0.39	0.70±0.17	0.86±0.73	0.86±0.42	1.02±0.38	6.07±1.76	17.00±6.58
SD	0.59±1.82	0.93±0.84	6.42±4.11	0.98±0.67	1.17±5.09	2.65±4.08	1.57±5.68	2.57±3.28	2.45±2.39	23.25±21.45
SD-T	0.63±2.40	0.60±0.96	3.82±4.98	0.96±0.64	1.21±5.03	3.40±4.99	3.02±5.02	2.36±3.90	1.52±3.43	20.09±23.88
SD-AT	0.52±2.42	0.60±0.95	3.18±5.10	0.96±0.64	1.24±5.00	3.93±5.03	2.22±5.04	2.00±3.91	1.80±3.39	18.90±24.15
SMc	0.87±2.05	0.63±0.77	1.38±6.00	1.02±0.49	1.41±5.28	2.02±4.36	1.94±5.72	2.91±4.94	2.32±2.31	22.47±20.80
SMc-A	1.02±2.22	0.47±0.77	3.92±3.91	0.91±0.55	2.32±5.23	3.54±4.98	2.74±5.30	5.96±4.59	2.23±3.82	27.82±18.82
SMc-T	0.57±1.79	0.69±0.35	1.28±3.73	0.93±0.49	0.80±4.51	0.99±4.01	1.20±4.68	1.40±3.91	1.81±0.83	13.43±19.27
SMc-AT	0.66±1.90	0.55±0.29	2.76±3.63	0.94±0.47	0.91±4.11	1.10±4.00	1.26±4.26	1.45±4.56	2.05±0.96	16.50±17.96
SMc-ATN	2.24±2.36	0.58±0.49	6.82±4.81	1.56±0.54	6.46±4.14	8.51±4.43	7.21±4.28	7.60±3.11	1.47±1.02	43.85±18.41
SMT	3.00±1.85	0.74±0.90	0.00±1.95	1.64±0.70	8.94±4.66	6.49±4.99	8.47±5.58	7.72±4.41	3.10±2.97	42.87
SMT-A	3.00±1.85	0.74±0.90	0.00±1.95	1.64±0.70	8.94±4.66	6.49±4.99	8.47±5.58	7.72±4.41	3.10±2.97	42.87
SMT-T	3.74±2.16	0.58±0.56	0.00±2.56	1.73±0.73	8.75±4.62	6.22±3.99	8.05±4.73	7.95±4.49	2.35±1.79	46.21±17.30
SMT-AT	3.74±2.16	0.58±0.56	0.00±2.56	1.73±0.73	8.75±4.62	6.22±3.99	8.05±4.73	7.95±4.49	2.35±1.79	46.21±17.30

266 We list the hyperparameters for the transformer SUNMASK models in the Appendix. Transformer
 267 SUNMASK was trained on every dataset used in this paper, and we show performance in Section 4,
 268 as well as comparisons to convolutional SUNMASK on symbolic polyphonic music modeling. Both
 269 convolutional and transformer based SUNMASK use the Adam optimizer, with gradient clipping by
 270 value at 3. Inference hyperparameter types and general sampling strategies used are the same with
 271 both models, though specific hyperparameter values may change between datasets.

272 4 Experiments

273 4.1 Quantitative Results

274 We demonstrate the use of SUNMASK for polyphonic symbolic music modeling on the JSB dataset [2,
 275 5]. The JSB dataset consists of 382 four-part chorales, originally written by Johann Sebastian Bach.
 276 These chorales are quantized at the 16th note interval, cut into non-overlapping chunks of length 128,
 277 skipping chunks which would cross the end of a piece. This processing results in a training dataset
 278 of 4956 examples, with each example being size (4, 128). We train convolutional and transformer
 279 versions of both SUNMASK and SUNDAE for comparison, as well as the pretrained Coconet [33].
 280 For polyphonic music, the quantized data was rasterized in soprano, alto, tenor, bass (SATB) order, as
 281 in Music Transformer [34] and BachBot [47], then chunked into non-overlapping training examples.
 282 Results are shown in Table 2. These results are evaluated on Bach ground truth data (Bach GT),
 283 BachMock Transformer (BachMock [19, 49]) (closely related to the decoder from VQ-CPC [28]),
 284 Coconet, SUNDAE (SD), and SUNMASK convolutional (SMc) and SUNMASK transformer (SMT).
 285 Model variants are indicated with Active Balance (A), Typical Sampling (T), and Noise (N).

286 The grading function used for evaluation, referred to as BachMock here, is designed specifically to
 287 correlate with expert analysis on Bach. In particular using this metric to choose correct examples in a
 288 paired comparison test, outperforms novice, intermediate, and expert listeners by varying margins [19].
 289 This indicates that scoring well on the aggregate metric should correlate to high sample quality. The
 290 metric has many sub-parts, ranking various musical attributes crucial to codifying the style of J.S.
 291 Bach. AugGen [49] incorporated this metric into an iterative training and sampling scheme which
 292 improved final generative capability for a fixed model, showing the effectiveness of BachMock in
 293 practice for ranking machine generated samples. For every grading function in Bach Mock grading
 294 function, we show the median value and \pm standard deviation as well as the overall grade, and lower
 295 values are better. We see the strongest results for convolutional SUNMASK with typicality sampling.
 296 Combined with final top-N ($N = 20$) selection out of a candidate set of 200 samples, the overall
 297 sample quality outperforms strong baselines. In addition, the massive performance gain from top-N
 298 selection indicates that the variance is likely driven by failures during sampling, rather than more
 299 fundamental modeling errors.

300 The EMNLP 2017 News dataset is a common benchmark for word-level language modeling [6],
 301 containing a large number of news article sentences [51]. Preprocessing steps collapse to sentences
 302 containing the most common 5700 words, resulting in a training set of 200k sentences with a test set
 303 of 10k. The overall maximum sentence length is 51. Common processing for this dataset includes

padding all sentences up to this maximum length, different than the standard long sequence chunking commonly used in other language modeling tasks.

We show the results of several SUNMASK models for generating sentences similar to EMNLP2017News, comparing to benchmarks using the standard Negative BLEU/Self-BLEU evaluation [80, 6] over generated corpora of 1000 sentences in Figure 2. This set of scores, varied across temperature, is compared against baseline scores [48, 78, 8, 26, 13, 75], similar to the evaluation shown in SUNDAE [65]. These reference benchmarks used 10000 sentences to form performance estimates.

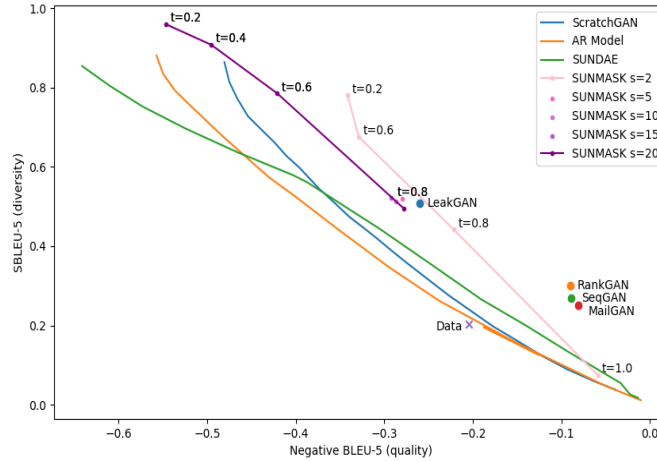


Figure 2: Negative BLEU/Self-BLEU scores on EMNLP2017 News. Left (x-axis) is better, lower (y-axis) is better. Quality/variation is controlled by changing the temperature (t), and varying diffusion schedule (s). For SUNMASK, typical sampling results [52] are shown.

311

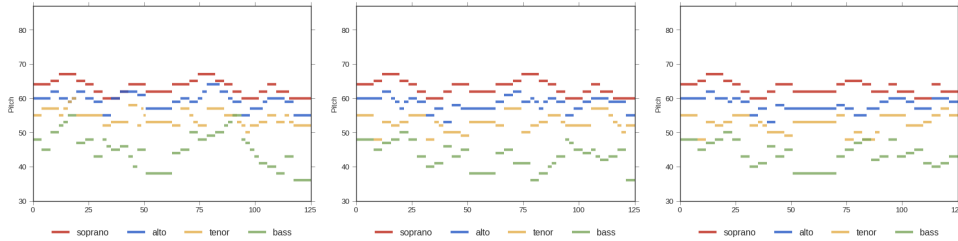


Figure 3: A

Figure 4: B

Figure 5: C

SUNMASK harmonization (bass, tenor, alto) of an existing melody (soprano)(A), with mask which highlights the left half (0 to 64) soprano voice (B), left half mask with right half replacement (C)

312 4.2 Qualitative Study of Masking For General Task Control

313 Given the flexibility of masking at inference, we perform a number of qualitative queries to inspect
 314 how the model adapts based on noise and mask value. Figures 3 4, and 5 demonstrate the use of
 315 SUNMASK for musical inpainting, holding the top voice (soprano) either fully or partially fixed to
 316 the well-known melody "Ode to Joy", by Ludwig van Beethoven. We see the trained model is more
 317 than capable of inpainting based on a pre-defined mask.

318 We test masks which hold the whole soprano fixed, masks which cover only parts of the soprano but
 319 do not allow randomization away from those notes, and masks which cover parts of the soprano but
 320 allow rewriting of the non-masked parts of the soprano, as well as rewriting all other voices. The use
 321 of masks to focus on subsets of variables while preserving underlying intermediate predictions is

322 unique to SUNMASK, as SUNDAE does not have an explicitly controllable input mask and Coconet
 323 does not have the ability to mask without also blanking the underlying variable.

324 This control is also demonstrated in Table 3, where masking is used to variably increase or decrease
 325 the weight on various pre-specified terms, held fixed throughout inference. The combination of these
 326 words, and their mask status can be seen to influence the overall tone of the selected text passages
 327 which showed the strongest effect in a particular inference batch. Though the generation quality is
 328 flawed, we clearly see a relationship between the masked word and the emergent surrounding context,
 329 for example highlighting **war** draws forth divorce, attack, and leave, while **play** instead references
 330 Premier Cup and excitement. We see similar results on a batch scale, and full demonstration of the
 331 text samples can be seen in the Appendix.

332 5 Conclusion

333 We introduce SUNMASK, a method for masked unrolled denoising modeling of structured data.
 334 SUNMASK separates the role of masking and correction by conditioning predictions on the mask,
 335 allowing for fine-grained control at inference. When applied to text as well as symbolic polyphonic
 336 music, SUNMASK is competitive with strong baselines, outperforming reference baselines on music
 337 modeling. Leveraging the separation of mask and noise allows for subtle control at inference, paving
 338 the way for a variety of domain specific applications and generative pipelines for human-in-the-loop
 339 creation.

Table 3: Qualitative samples using masks to emphasize the influence of particular words.
 Samples from a SUNMASK Transformer trained on the word level EMNLP2017News dataset.

Success unmasked <i>disaster</i> masked	I think I want to leave success at the end of the <i>disaster</i> , but because that ' s a nice to say it ' s not good to be the challenge and this is a very good thing <eos> That was the job I was success to have to pay my <i>disaster</i> but hopefully I have been able to pull playing in the first couple of the season , I ' ve been happy to go through this team , he said <eos>
<i>Success</i> masked disaster unmasked	Although more than 80 , 000 <i>success</i> have been displaced in the disaster since the last year , more than 700 , 000 lives have been injured in the country , and 70 of them were killed , according to the UN media <eos> I haven ' t had a <i>success</i> at the league , the disaster and picked running with the door ago we have Champions , and I was a couple of pressure . . . and it was a lot of times <eos>
Celebration unmasked <i>crime</i> masked	This is a fact on the celebration is such a really good <i>crime</i> , but it can be some of the most good people around the world and I think it must be the good way to do it <eos> It ' s part of those celebration at the start of the <i>crime</i> , and it ' s a lot of good pride over the past few years , it ' s going to be more happy to play through this world <eos>
<i>Celebration</i> masked crime unmasked	Last year , the numbers of <i>celebration</i> applications have been adopted in crime since the Middle since since year has watched a rate of more than 95 per cent in the UK since 2011 , 2015 to 45 per cent <eos> The Prime Minister has been a <i>celebration</i> to the course of the crime deal which and to have a relationship of the European Union , with the rest of the European Union has before the scandal <eos>
War unmasked <i>play</i> masked	The Prime Minister David Cameron said war had not be hard to <i>play</i> the divorce of the European Union , and determined it would mark a divorce between the majority of the UK and leave the bloc of the European Union <eos> It may be really more special war . . . try to <i>play</i> it , and I hope we ' re going to be able to attack this team so we have to do it <eos>
<i>War</i> masked play unmasked	But I was proud of the <i>war</i> I ' ve got to play to it but I wish that ' s because I want to do , and I ' m pretty excited before the end of the season , he said <eos> We are in the Premier Cup <i>war</i> and we want to keep play with their top six that which we need to play in the World Champions and at the end of the season that we have to be it well <eos>
Unconstrained generations	By the time , the driver had been deployed to lie out to the incident , an new official said that the woman had not been found a them <eos> According to The Wall Post survey poll found that 80 per cent of eligible older registered who , they thought he would be the rate for 10 per cent less likely to vote , while 16 per cent of those said they would still less likely to happen <eos>

340 References

- 341 [1] Guillaume Alain and Yoshua Bengio. What regularized auto-encoders learn from the data-
342 generating distribution. *The Journal of Machine Learning Research*, 15(1):3563–3593, 2014.
- 343 [2] Moray Allan and Christopher Williams. Harmonising chorales by probabilistic inference.
344 *Advances in neural information processing systems*, 17, 2004.
- 345 [3] Jacob Austin, Daniel D Johnson, Jonathan Ho, Daniel Tarlow, and Rianne van den Berg.
346 Structured denoising diffusion models in discrete state-spaces. *Advances in Neural Information*
347 *Processing Systems*, 34:17981–17993, 2021.
- 348 [4] Philip Bachman and Doina Precup. Data generation as sequential decision making. *Advances*
349 *in Neural Information Processing Systems*, 28, 2015.
- 350 [5] Nicolas Boulanger-Lewandowski, Yoshua Bengio, and Pascal Vincent. Modeling temporal
351 dependencies in high-dimensional sequences: application to polyphonic music generation and
352 transcription. In *Proceedings of the 29th International Conference on International Conference*
353 *on Machine Learning*, pages 1881–1888, 2012.
- 354 [6] Massimo Caccia, Lucas Caccia, William Fedus, Hugo Larochelle, Joelle Pineau, and Laurent
355 Charlin. Language gans falling short. *arXiv preprint arXiv:1811.02549*, 2018.
- 356 [7] Huiwen Chang, Han Zhang, Lu Jiang, Ce Liu, and William T. Freeman. Maskgit: Masked
357 generative image transformer. In *The IEEE Conference on Computer Vision and Pattern*
358 *Recognition (CVPR)*, June 2022.
- 359 [8] Tong Che, Yanran Li, Ruixiang Zhang, R Devon Hjelm, Wenjie Li, Yangqiu Song, and Yoshua
360 Bengio. Maximum-likelihood augmented discrete generative adversarial networks. *arXiv*
361 *preprint arXiv:1702.07983*, 2017.
- 362 [9] Nanxin Chen, Yu Zhang, Heiga Zen, Ron J Weiss, Mohammad Norouzi, and William Chan.
363 Wavegrad: Estimating gradients for waveform generation. In *International Conference on*
364 *Learning Representations*, 2020.
- 365 [10] Kevin Clark, Minh-Thang Luong, Quoc V Le, and Christopher D Manning. Electra: Pre-training
366 text encoders as discriminators rather than generators. *arXiv preprint arXiv:2003.10555*, 2020.
- 367 [11] Katherine Crowson, Stella Biderman, Daniel Kornis, Dashiell Stander, Eric Hallahan, Louis
368 Castricato, and Edward Raff. Vqgan-clip: Open domain image generation and editing with
369 natural language guidance, 2022.
- 370 [12] Zihang Dai, Zhilin Yang, Yiming Yang, Jaime Carbonell, Quoc V Le, and Ruslan Salakhutdinov.
371 Transformer-xl: Attentive language models beyond a fixed-length context. *arXiv preprint*
372 *arXiv:1901.02860*, 2019.
- 373 [13] Cyprien de Masson d’Autume, Shakir Mohamed, Mihaela Rosca, and Jack Rae. Training
374 language gans from scratch. *Advances in Neural Information Processing Systems*, 32, 2019.
- 375 [14] Jacob Devlin, Ming-Wei Chang, Kenton Lee, and Kristina Toutanova. Bert: Pre-training of
376 deep bidirectional transformers for language understanding. *arXiv preprint arXiv:1810.04805*,
377 2018.
- 378 [15] Laurent Dinh, David Krueger, and Yoshua Bengio. Nice: Non-linear independent components
379 estimation. *arXiv preprint arXiv:1410.8516*, 2014.
- 380 [16] Laurent Dinh, Jascha Sohl-Dickstein, and Samy Bengio. Density estimation using real nvp.
381 *arXiv preprint arXiv:1605.08803*, 2016.
- 382 [17] Chris Donahue, Mina Lee, and Percy Liang. Enabling language models to fill in the blanks.
383 *arXiv preprint arXiv:2005.05339*, 2020.
- 384 [18] Patrick Esser, Robin Rombach, and Bjorn Ommer. Taming transformers for high-resolution
385 image synthesis. In *Proceedings of the IEEE/CVF Conference on Computer Vision and Pattern*
386 *Recognition (CVPR)*, pages 12873–12883, June 2021.

- 387 [19] Alexander Fang, Alisa Liu, Prem Seetharaman, and Bryan Pardo. Bach or mock? a grading
388 function for chorales in the style of js bach. *arXiv preprint arXiv:2006.13329*, 2020.
- 389 [20] William Fedus, Ian Goodfellow, and Andrew M. Dai. Maskgan: Better text generation via
390 filling in the _____, 2018.
- 391 [21] Yaroslav Ganin, Tejas Kulkarni, Igor Babuschkin, SM Ali Eslami, and Oriol Vinyals. Synthe-
392 sizing programs for images using reinforced adversarial learning. In *International Conference*
393 *on Machine Learning*, pages 1666–1675. PMLR, 2018.
- 394 [22] Mathieu Germain, Karol Gregor, Iain Murray, and Hugo Larochelle. Made: Masked autoencoder
395 for distribution estimation. In *International Conference on Machine Learning*, pages 881–889.
396 PMLR, 2015.
- 397 [23] Ian Goodfellow, Jean Pouget-Abadie, Mehdi Mirza, Bing Xu, David Warde-Farley, Sherjil
398 Ozair, Aaron Courville, and Yoshua Bengio. Generative adversarial nets. *Advances in neural*
399 *information processing systems*, 27, 2014.
- 400 [24] Karol Gregor, Ivo Danihelka, Alex Graves, Danilo Rezende, and Daan Wierstra. Draw: A
401 recurrent neural network for image generation. In *International Conference on Machine*
402 *Learning*, pages 1462–1471. PMLR, 2015.
- 403 [25] Shuyang Gu, Dong Chen, Jianmin Bao, Fang Wen, Bo Zhang, Dongdong Chen, Lu Yuan, and
404 Baining Guo. Vector quantized diffusion model for text-to-image synthesis. *arXiv preprint*
405 *arXiv:2111.14822*, 2021.
- 406 [26] Junliang Guo, Linli Xu, and Enhong Chen. Jointly masked sequence-to-sequence model for
407 non-autoregressive neural machine translation. In *Proceedings of the 58th Annual Meeting of*
408 *the Association for Computational Linguistics*, pages 376–385, 2020.
- 409 [27] Michael Gutmann and Aapo Hyvärinen. Noise-contrastive estimation: A new estimation
410 principle for unnormalized statistical models. In *Proceedings of the thirteenth international con-*
411 *ference on artificial intelligence and statistics*, pages 297–304. JMLR Workshop and Conference
412 Proceedings, 2010.
- 413 [28] Gaëtan Hadjeres and Léopold Crestel. Vector quantized contrastive predictive coding for
414 template-based music generation. *arXiv preprint arXiv:2004.10120*, 2020.
- 415 [29] Kaiming He, Xinlei Chen, Saining Xie, Yanghao Li, Piotr Dollár, and Ross Girshick. Masked
416 autoencoders are scalable vision learners. *arXiv:2111.06377*, 2021.
- 417 [30] Jonathan Ho, Ajay Jain, and Pieter Abbeel. Denoising diffusion probabilistic models. *Advances*
418 *in Neural Information Processing Systems*, 33:6840–6851, 2020.
- 419 [31] Emiel Hoogeboom, Alexey A Gritsenko, Jasmijn Bastings, Ben Poole, Rianne van den Berg,
420 and Tim Salimans. Autoregressive diffusion models. *arXiv preprint arXiv:2110.02037*, 2021.
- 421 [32] Emiel Hoogeboom, Didrik Nielsen, Priyank Jaini, Patrick Forré, and Max Welling. Argmax
422 flows and multinomial diffusion: Learning categorical distributions. *Advances in Neural*
423 *Information Processing Systems*, 34, 2021.
- 424 [33] Cheng-Zhi Anna Huang, Tim Cooijmans, Adam Roberts, Aaron Courville, and Douglas Eck.
425 Counterpoint by convolution. *arXiv preprint arXiv:1903.07227*, 2019.
- 426 [34] Cheng-Zhi Anna Huang, Ashish Vaswani, Jakob Uszkoreit, Ian Simon, Curtis Hawthorne,
427 Noam Shazeer, Andrew M Dai, Matthew D Hoffman, Monica Dinculescu, and Douglas Eck.
428 Music transformer: Generating music with long-term structure. In *International Conference on*
429 *Learning Representations*, 2018.
- 430 [35] Chin-Wei Huang, Jae Hyun Lim, and Aaron C Courville. A variational perspective on diffusion-
431 based generative models and score matching. *Advances in Neural Information Processing*
432 *Systems*, 34, 2021.

- 433 [36] Rongjie Huang, Max WY Lam, Jun Wang, Dan Su, Dong Yu, Yi Ren, and Zhou Zhao. Fast-
434 diff: A fast conditional diffusion model for high-quality speech synthesis. *arXiv preprint*
435 *arXiv:2204.09934*, 2022.
- 436 [37] Daphne Ippolito, Anna Huang, Curtis Hawthorne, and Douglas Eck. Infilling piano perfor-
437 mances. In *NIPS Workshop on Machine Learning for Creativity and Design*, 2018.
- 438 [38] Nal Kalchbrenner, Ivo Danihelka, and Alex Graves. Grid long short-term memory. *arXiv*
439 *preprint arXiv:1507.01526*, 2015.
- 440 [39] Nal Kalchbrenner, Erich Elsen, Karen Simonyan, Seb Noury, Norman Casagrande, Edward
441 Lockhart, Florian Stimberg, Aaron Oord, Sander Dieleman, and Koray Kavukcuoglu. Efficient
442 neural audio synthesis. In *International Conference on Machine Learning*, pages 2410–2419.
443 PMLR, 2018.
- 444 [40] Diederik P Kingma, Tim Salimans, Ben Poole, and Jonathan Ho. Variational diffusion models.
445 In *Advances in Neural Information Processing Systems*, 2021.
- 446 [41] Diederik P Kingma and Max Welling. Auto-encoding variational bayes. *arXiv preprint*
447 *arXiv:1312.6114*, 2013.
- 448 [42] Durk P Kingma, Tim Salimans, Rafal Jozefowicz, Xi Chen, Ilya Sutskever, and Max Welling.
449 Improved variational inference with inverse autoregressive flow. *Advances in neural information*
450 *processing systems*, 29, 2016.
- 451 [43] Zhifeng Kong, Wei Ping, Jiaji Huang, Kexin Zhao, and Bryan Catanzaro. Diffwave: A versatile
452 diffusion model for audio synthesis. In *International Conference on Learning Representations*,
453 2020.
- 454 [44] Max WY Lam, Jun Wang, Rongjie Huang, Dan Su, and Dong Yu. Bilateral denoising diffusion
455 models. *arXiv preprint arXiv:2108.11514*, 2021.
- 456 [45] Alex M Lamb, Devon Hjelm, Yaroslav Ganin, Joseph Paul Cohen, Aaron C Courville, and
457 Yoshua Bengio. Gibbsnet: Iterative adversarial inference for deep graphical models. *Advances*
458 *in Neural Information Processing Systems*, 30, 2017.
- 459 [46] Jason Lee, Elman Mansimov, and Kyunghyun Cho. Deterministic non-autoregressive neural
460 sequence modeling by iterative refinement. In *EMNLP*, 2018.
- 461 [47] Feynman Liang. Bachbot: Automatic composition in the style of bach chorales. *University of*
462 *Cambridge*, 8:19–48, 2016.
- 463 [48] Kevin Lin, Dianqi Li, Xiaodong He, Zhengyou Zhang, and Ming-Ting Sun. Adversarial ranking
464 for language generation. *Advances in neural information processing systems*, 30, 2017.
- 465 [49] Alisa Liu, Alexander Fang, Gaëtan Hadjeres, Prem Seetharaman, and Bryan Pardo. Incorporat-
466 ing music knowledge in continual dataset augmentation for music generation. *arXiv preprint*
467 *arXiv:2006.13331*, 2020.
- 468 [50] Yinhan Liu, Myle Ott, Naman Goyal, Jingfei Du, Mandar Joshi, Danqi Chen, Omer Levy, Mike
469 Lewis, Luke Zettlemoyer, and Veselin Stoyanov. Roberta: A robustly optimized bert pretraining
470 approach. *arXiv preprint arXiv:1907.11692*, 2019.
- 471 [51] Sidi Lu, Yaoming Zhu, Weinan Zhang, Jun Wang, and Yong Yu. Neural text generation: Past,
472 present and beyond. *arXiv preprint arXiv:1803.07133*, 2018.
- 473 [52] Clara Meister, Tiago Pimentel, Gian Wiher, and Ryan Cotterell. Typical decoding for natural
474 language generation. *arXiv preprint arXiv:2202.00666*, 2022.
- 475 [53] Chenlin Meng, Yang Song, Jiaming Song, Jiajun Wu, Jun-Yan Zhu, and Stefano Ermon.
476 Sdedit: Image synthesis and editing with stochastic differential equations. *arXiv preprint*
477 *arXiv:2108.01073*, 2021.
- 478 [54] Gautam Mittal, Jesse Engel, Curtis Hawthorne, and Ian Simon. Symbolic music generation
479 with diffusion models. *arXiv preprint arXiv:2103.16091*, 2021.

- 480 [55] Alex Nichol. Vq-draw: A sequential discrete vae. *arXiv preprint arXiv:2003.01599*, 2020.
- 481 [56] Alex Nichol, Prafulla Dhariwal, Aditya Ramesh, Pranav Shyam, Pamela Mishkin, Bob McGrew,
482 Ilya Sutskever, and Mark Chen. Glide: Towards photorealistic image generation and editing
483 with text-guided diffusion models. *arXiv preprint arXiv:2112.10741*, 2021.
- 484 [57] George Papamakarios, Theo Pavlakou, and Iain Murray. Masked autoregressive flow for density
485 estimation. *Advances in neural information processing systems*, 30, 2017.
- 486 [58] Ashis Pati, Alexander Lerch, and Gaëtan Hadjeres. Learning to traverse latent spaces for
487 musical score inpainting. *arXiv preprint arXiv:1907.01164*, 2019.
- 488 [59] Christine Payne. Musenet. *openai.com/blog/musenet*, 2019.
- 489 [60] Aditya Ramesh, Prafulla Dhariwal, Alex Nichol, Casey Chu, and Mark Chen. Hierarchical
490 text-conditional image generation with clip latents, 2022.
- 491 [61] Danilo Rezende and Shakir Mohamed. Variational inference with normalizing flows. In
492 *International conference on machine learning*, pages 1530–1538. PMLR, 2015.
- 493 [62] Robin Rombach, Andreas Blattmann, Dominik Lorenz, Patrick Esser, and Björn Ommer.
494 High-resolution image synthesis with latent diffusion models, 2021.
- 495 [63] Chitwan Saharia, William Chan, Huiwen Chang, Chris A Lee, Jonathan Ho, Tim Salimans,
496 David J Fleet, and Mohammad Norouzi. Palette: Image-to-image diffusion models. *arXiv*
497 *preprint arXiv:2111.05826*, 2021.
- 498 [64] Chitwan Saharia, Jonathan Ho, William Chan, Tim Salimans, David J Fleet, and Mohammad
499 Norouzi. Image super-resolution via iterative refinement. *arXiv preprint arXiv:2104.07636*,
500 2021.
- 501 [65] Nikolay Savinov, Junyoung Chung, Mikolaj Binkowski, Erich Elsen, and Aaron van den Oord.
502 Step-unrolled denoising autoencoders for text generation. *arXiv preprint arXiv:2112.06749*,
503 2021.
- 504 [66] Raphael Shu, Jason Lee, Hideki Nakayama, and Kyunghyun Cho. Latent-variable non-
505 autoregressive neural machine translation with deterministic inference using a delta posterior.
506 In *Proceedings of the AAAI Conference on Artificial Intelligence*, volume 34, pages 8846–8853,
507 2020.
- 508 [67] Jascha Sohl-Dickstein, Eric Weiss, Niru Maheswaranathan, and Surya Ganguli. Deep unsuper-
509 vised learning using nonequilibrium thermodynamics. In *International Conference on Machine*
510 *Learning*, pages 2256–2265. PMLR, 2015.
- 511 [68] Yang Song, Conor Durkan, Iain Murray, and Stefano Ermon. Maximum likelihood training of
512 score-based diffusion models. *Advances in Neural Information Processing Systems*, 34, 2021.
- 513 [69] Yang Song and Stefano Ermon. Generative modeling by estimating gradients of the data
514 distribution. *Advances in Neural Information Processing Systems*, 32, 2019.
- 515 [70] Lucas Theis and Matthias Bethge. Generative image modeling using spatial lstms. *Advances in*
516 *neural information processing systems*, 28, 2015.
- 517 [71] Benigno Uribe, Marc-Alexandre Côté, Karol Gregor, Iain Murray, and Hugo Larochelle. Neural
518 autoregressive distribution estimation. *The Journal of Machine Learning Research*, 17(1):7184–
519 7220, 2016.
- 520 [72] Benigno Uribe, Iain Murray, and Hugo Larochelle. A deep and tractable density estimator. In
521 *International Conference on Machine Learning*, pages 467–475. PMLR, 2014.
- 522 [73] Aaron Van Oord, Nal Kalchbrenner, and Koray Kavukcuoglu. Pixel recurrent neural networks.
523 In *International conference on machine learning*, pages 1747–1756. PMLR, 2016.
- 524 [74] Sean Vasquez and Mike Lewis. Melnet: A generative model for audio in the frequency domain.
525 *arXiv preprint arXiv:1906.01083*, 2019.

- 526 [75] Ashish Vaswani, Noam Shazeer, Niki Parmar, Jakob Uszkoreit, Llion Jones, Aidan N Gomez,
527 Łukasz Kaiser, and Illia Polosukhin. Attention is all you need. *Advances in neural information*
528 *processing systems*, 30, 2017.
- 529 [76] Francesco Visin, Kyle Kastner, Kyunghyun Cho, Matteo Matteucci, Aaron Courville, and
530 Yoshua Bengio. Renet: A recurrent neural network based alternative to convolutional networks.
531 *arXiv preprint arXiv:1505.00393*, 2015.
- 532 [77] Zhilin Yang, Zihang Dai, Yiming Yang, Jaime Carbonell, Russ R Salakhutdinov, and Quoc V
533 Le. Xlnet: Generalized autoregressive pretraining for language understanding. *Advances in*
534 *neural information processing systems*, 32, 2019.
- 535 [78] Lantao Yu, Weinan Zhang, Jun Wang, and Yong Yu. Seqgan: Sequence generative adversarial
536 nets with policy gradient. In *Proceedings of the AAAI conference on artificial intelligence*,
537 volume 31, 2017.
- 538 [79] Qinsheng Zhang and Yongxin Chen. Fast sampling of diffusion models with exponential
539 integrator. *arXiv preprint arXiv:2204.13902*, 2022.
- 540 [80] Yaoming Zhu, Sidi Lu, Lei Zheng, Jiaxian Guo, Weinan Zhang, Jun Wang, and Yong Yu.
541 Taxygen: A benchmarking platform for text generation models. In *The 41st International ACM*
542 *SIGIR Conference on Research & Development in Information Retrieval*, pages 1097–1100,
543 2018.

544 Checklist

- 545 1. For all authors...
- 546 (a) Do the main claims made in the abstract and introduction accurately reflect the paper’s
547 contributions and scope? **[TODO][Yes]**
- 548 (b) Did you describe the limitations of your work? **[TODO][Yes]** Throughout the paper
549 we list downsides to including the mask in the input, as well as the complexity of our
550 inference pipeline
- 551 (c) Did you discuss any potential negative societal impacts of your work? **[TODO][Yes]**
552 We plan to address this in the supplementary material and appendix due to space
553 limitations
- 554 (d) Have you read the ethics review guidelines and ensured that your paper conforms to
555 them? **[TODO][Yes]**
- 556 2. If you are including theoretical results...
- 557 (a) Did you state the full set of assumptions of all theoretical results? **[TODO][Yes]** Our
558 theorems state the relevant conditions
- 559 (b) Did you include complete proofs of all theoretical results? **[TODO][Yes]** We also cite
560 relevant prior work on said theorems
- 561 3. If you ran experiments...
- 562 (a) Did you include the code, data, and instructions needed to reproduce the main experi-
563 mental results (either in the supplemental material or as a URL)? **[TODO][No]** We will
564 include a (likely non-runnable) version of the experimental code in the supplemental
565 material, and work toward a more generally usable release during the review cycle
- 566 (b) Did you specify all the training details (e.g., data splits, hyperparameters, how they
567 were chosen)? **[TODO][No]** To fully disclose this, requires full experimental code
- 568 (c) Did you report error bars (e.g., with respect to the random seed after running experi-
569 ments multiple times)? **[TODO][Yes]** Variance in the scoring table
- 570 (d) Did you include the total amount of compute and the type of resources used (e.g., type
571 of GPUs, internal cluster, or cloud provider)? **[TODO][No]** We discuss the GPU type,
572 but do not do a full accounting of resources used. All experiments were trained on
573 commodity hardware (P100/V100/A100) using single GPUs, for less than 24 hours an
574 experiment run
- 575 4. If you are using existing assets (e.g., code, data, models) or curating/releasing new assets...

- 576 (a) If your work uses existing assets, did you cite the creators? **[TODO]**[Yes]
577 (b) Did you mention the license of the assets? **[TODO]**[No] All material is extensively
578 used in prior work
579 (c) Did you include any new assets either in the supplemental material or as a URL?
580 **[TODO]**[No] No new assets
581 (d) Did you discuss whether and how consent was obtained from people whose data you're
582 using/curating? **[TODO]**[No] No new assets, and assets used are public domain
583 (e) Did you discuss whether the data you are using/curating contains personally identifiable
584 information or offensive content? **[TODO]**[No]
585 5. If you used crowdsourcing or conducted research with human subjects...
586 (a) Did you include the full text of instructions given to participants and screenshots, if
587 applicable? **[TODO]**[N/A]
588 (b) Did you describe any potential participant risks, with links to Institutional Review
589 Board (IRB) approvals, if applicable? **[TODO]**[N/A]
590 (c) Did you include the estimated hourly wage paid to participants and the total amount
591 spent on participant compensation? **[TODO]**[N/A]